Connection Performance of Mass Plywood Panels

Byrne T. Miyamoto
Arijit Sinha
Ian Morrell

Abstract

Tall wood buildings have become more prevalent in North America in the past 10 years. Tall wood-frame buildings implement both mass timber construction and products. Mass timber products are wood-based products that can withstand and hold large loads for long durations of time. Mass timber has allowed for large buildings, which consist mainly of wood, to be erected comprising multiple stories. One new mass timber product that has been fashioned is Mass Plywood Panels (MPP). MPP is a veneer-based engineered wood product, which is a massive, large-scale, structural composite lumber–based panel designed for use in building applications as both a vertical and horizontal element. For any new product to be used in the industry with confidence, a thorough investigation of its physical, mechanical, and connection properties is needed. A series of connection tests, such as fastener withdrawal resistance, dowel-bearing strength, lateral resistance, and a component test on a wall-to-floor system were conducted. The lateral resistance test indicated that the current European Yield Models can be used to calculate the yield loads and yield mode of the MPP by using the dowel-bearing strength of plywood. Three different connection configurations were tested in two distinct loading directions—shear and withdrawal. Their performances are evaluated and compared using two existing engineering models—namely, the American Society of Civil Engineers 41-13 tri-linear model and the seismic analysis of wood-frame structures 10-parameter connection model.

In North America, tall wood buildings are gaining traction in cities. Tall wood buildings implement both mass timber construction and mass timber products. Mass timber construction is a building process that uses engineered wood products as the primary structural material (Kremer and Symmons 2015). These engineered wood products used in mass timber construction consist of cross-laminated timber (CLT), nail-laminated timber (nail-lam), glued-laminated timber (glulam), and dowel-laminated timber, to name a few examples. CLT and glulam are two of the most used mass timber products in construction. One new product that has been developed is Mass Plywood Panels (MPP).

MPP was developed and is produced by Freres Lumber Co., Inc., located in Lyons, Oregon. MPP is a veneer-based engineered wood product, which is a massive, large-scale, structural composite lumber–based engineered wood product. MPP consists of multiple veneer-based structural composite lumber panels stacked together and adhered with structural grade adhesive. MPP can be manufactured with dimensions up to 3.7 m wide by 14.6 m long with a maximum thickness of 0.6 m. A typical MPP panel is laid up with two face panels and a selected number of core panels based on the desired thickness. The face and core panels contain different ply configurations to optimize properties for its intended end use. Face panels have the plies oriented in a manner that allows the panel to have a greater stiffness in the longitudinal direction, while the core panels have cross-banding that increases the dimensional stability of the MPP.

As an engineered wood product consisting of veneer-based structural composites panels, MPP has many characteristics of plywood. The naturally occurring defects are reduced and smaller defects are spread throughout the MPP because of the different orientations of veneers and multiple plies. Plywood has high strength-to-weight and strength-to-thickness ratios that should translate to MPP (Forest Products Laboratory [FPL] 2010). The alteration of the grain direction in plywood gives it dimensional stability,

The authors are, respectively, Graduate Research Assistant, Associate Professor, and Graduate Research Assistant, Dept. of Wood Sci., Oregon State Univ., Corvallis (byrne.miyamoto@oregonstate.edu, Arijit.sinha@oregonstate.edu [corresponding author], ian.morrell@oregonstate.edu). This paper was received for publication in October 2019. Article no. 19-00056.

Forest Prod. J. 70(1):88–99.
doi:10.13073/FPJ-D-19-00056

reduces edge swelling, and reduces splitting when applying fasteners near the edge (FPL 2010).

MPP and CLT can be applied in similar locations in a building. MPP can be used in both wall and flooring systems in residential and nonresidential applications. MPP has successfully attained third-party certification, and its flexural and shear properties as a function of number of layup is listed in the Product Report (PR-L325) published by the Engineered Wood Association (APA 2018). To expand the knowledge base of MPP, as well as certify it for structural use, the authors are in the process of comprehensively characterizing standard properties, such as flexure, shear, in-plane shear, and tension, which will be part of a future publication. Apart from standard properties, connection properties for new products such as MPP must be characterized for it to be used with confidence.

MPP is a new product, so a plethora of experimental data is needed to characterize its basic connection properties such as withdrawal, dowel-bearing strength, and lateral nail resistance. These properties are well understood in wood and plywood (FPL 2010, American Wood Council [AWC] 2018). For the MPP panels to act in an assembly, connections between horizontal and vertical panels must be studied. These connections are achieved through angled brackets, which have been commonly used for CLT connection in Europe. The connection performance for conventional CLT products has been investigated in several studies (Gavric et al. 2011; Ceccotti et al. 2013; Pei et al. 2013; Rinaldin et al. 2013; Kramer et al. 2015; Mahdavifar et al. 2016, 2018). Mahdavifar et al. (2019) studied these bracket types with regular and hybrid CLT panels. Another viable option is to use self-tapping screws (STS) at an angle to achieve these connections. Although STS has been studied previously for use with CLT panels, there is a lack of information about its use with MPP.

This study investigates various connection properties of MPP. First, withdrawal tests in three different directions with respect to grain angle were conducted. Second, the yield strengths of laterally loaded, single fastener connections were evaluated. Finally, three different connection types were evaluated for two primary directions of loading—shear and withdrawal—with respect to the fasteners. The specific objectives of this study were as follows:

1. To characterize basic connection properties of MPP. Specifically,
   a. To study the withdrawal capacities of dowel type fasteners in MPP, and
   b. To determine yield strengths of laterally loaded single fastener connections with MPP, and
   c. To determine dowel-bearing strength of MPP in three different orientations.
2. To study the behavior of three different connection systems under cyclic loads in two predominant loading directions—lateral (shear) and withdrawal.

Materials and Methods

The MPP was procured from Freres Lumber Co., Inc., Lyons, Oregon. The thickness of MPP was 76.2 mm. The MPP panels had a moisture content of approximately 12 percent with a specific gravity (SG) of 0.53 determined using an ovendrying method. The MPP consisted of three layers of 25.4-mm-thick structural composite lumber, which contained nine Douglas-fir (*Pseudotsuga menziesii*) veneers per sheet. The veneer orientations of the face sheets differed from the core sheet. The face sheets of the MPP were oriented with approximately 80 percent of the plies in the strong axis, while the core sheet had the plies oriented equally in both directions. A sample typical MPP configuration is illustrated in Figure 1. A summary of the test matrix is provided in Table 1 along with the dimensions of the specimens.

Withdrawal

Tests were conducted following ASTM Standard D1761, methods for mechanical fasteners in wood (ASTM International 2012). Three fastener types were selected—8D smooth shank nails, Simpson StrongTie CNA 4 by 60 annular ring shank nails, and Simpson StrongTie SDS25300 wood screws. Nails were 3.3 mm in diameter and 65 mm in length, while screws were 6.4 mm in diameter and 76.2 mm in length. The fasteners were installed into the specimen in three orientations (Fig. 1). Six specimens were tested per orientation, for 18 total specimens per fastener type.

Tests were conducted on an INSTRON Universal Testing Machine (UTM). A gripping head connected to the crossarm of the UTM gripped the fastener head and was displaced at a rate of 5 mm/min (monotonic). The crossarm displacement and force were recorded to produce a load-deflection curve. The maximum load was recorded once the fastener had been withdrawn.

Lateral resistance

Tests were conducted on MPP following ASTM Standard D1761 for methods for mechanical fasteners in wood (ASTM International 2012). Similar fasteners as used in withdrawal tests were used in the lateral resistance tests. The specimen consisted of an MPP main member with a metal-plate side member connected by one fastener. The screws were installed through a 14-gauge (1.9-mm) galvanized-steel Grade 33 metal sheet, while the nails used a 10-gage (3.4-mm) galvanized-steel Grade 33 metal sheet. The metal plates were drilled at 12.7 and 25.4 mm from the sides and end of the plate, respectively. The fasteners were tested at three different orientations between the metal plate and MPP (Fig. 2). Orientations A and B had fasteners oriented

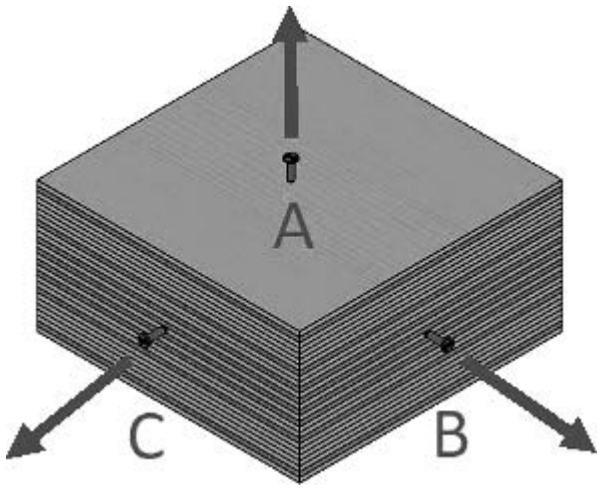

Figure 1.—Illustration of Mass Plywood Panels (MPP) sample and withdrawal orientations

Table 1.—Specimen dimensions and number of tests conducted.

Test	Thickness (mm)	Width (mm)	Length (m)	No.
Withdrawal				
Orientations A, B, and C	76.2	152.4	0.15	36
Lateral resistance				
Orientations A, B, and C	76.2	152.4	0.15	36
Dowel bearing (25.4-mm bolt)				
Orientation A	76.2	101.6	0.08	6
Orientation B	76.2	101.6	0.08	6
Dowel bearing (12.7-mm bolt)				
Orientation A	76.2	101.6	0.08	6
Orientation B	76.2	101.6	0.08	6
Dowel bearing (screw)				
Orientation A	76.2	101.6	0.05	6
Orientation B	76.2	101.6	0.05	6
Orientation C	76.2	76.2	0.06	6
Dowel bearing (nail)				
Orientation A	76.2	101.6	0.05	6
Orientation B	76.2	101.6	0.05	6
Orientation C	50.8	76.2	0.05	6
Shear components				
Floor	76.2	304.8	0.30	18
Wall	76.2	266.7	0.25	
Withdrawal components				
Floor	76.2	203.2	0.48	18
Wall	76.2	406.4	0.25	

perpendicular to the face veneer, while the force applied was parallel and perpendicular to the grain direction of the face veneer, respectively. Orientation C had the fastener oriented parallel to the laminations, while the force was applied in the grain direction of the face plies. The MPP was clamped to the base of the UTM, while a gripping head was clamped to the metal plate. The specimens were loaded monotonically at a rate of 5 mm/min until the load-deflection curve, being monitored for the test, leveled off.

Dowel bearing

Dowel-bearing tests were conducted following ASTM Standard D5764 for evaluating dowel-bearing strength of wood and wood-based products (ASTM International 2018). Tests included four different dowel sizes, with diameters of 25.4, 12.7, 6.3, and 4.3 mm. The 6.3- and 4.3-mm diameters represented the screw and nail, respectively, while the 25.4- and 12.7-mm diameters represented potential use of bolts. The specimens were prepared with a half-hole machined into the member along three possible grain orientations. The nail and screw specimens were tested in three orientations (A, B, and C), while the bolts were tested in two orientations (A and B), as illustrated in Figure 3.

The specimens were placed on a pivoting base with the dowel placed into the half-hole, which was centered under the load head. The load head consisted of a steel compression plate that applied a compressive force onto the metal dowel. The cross-arm applied displacement at a rate of 1 mm/min until the loading plate made complete contact with the sample surface, at which point the dowel was completely embedded into the sample.

Lateral connections and dowel-bearing calulations

To calculate the yield and dowel-bearing strength, the load deflection curves for each test were used. The yield load was calculated using the 5 percent offset method (Fig. 4). To calculate the 5 percent offset, the linear portion of the line was first defined by conducting regression fits on the data set until the correlation close to the unity was achieved. Once correlation was satisfied, a line parallel to the linear portion of the curve was offset by 5 percent of the dowel diameter. The yield point (P-yield) of the connection or the dowel-bearing tests was defined as the intersection of the 5 percent offset line and the load-deflection curve (AWC 2015).

Yield strength predictions

The predicted yield strengths and modes for the lateral resistance test were calculated using the AWC Technical Report 12, table 1-1 (AWC 2015). These equations, commonly known in the United States as the European Yield Model (EYM), and world-wide as Johansen's yield models, are well documented in AWC (2015). Using the equations in the AWC Technical Report, EYM calculates six possible ways the connection can yield. These equations calculate all possible yield strengths and modes. The lowest yield strength is then taken and adjusted using adjustment factors found in the National Design Specification (NDS; AWC 2018). Once adjusted, this value becomes the yield strength and the corresponding mode is the yield mode. The EYM has seven inputs: dowel-bearing strength for the side and main member, dowel diameter, gap, side-member dowel

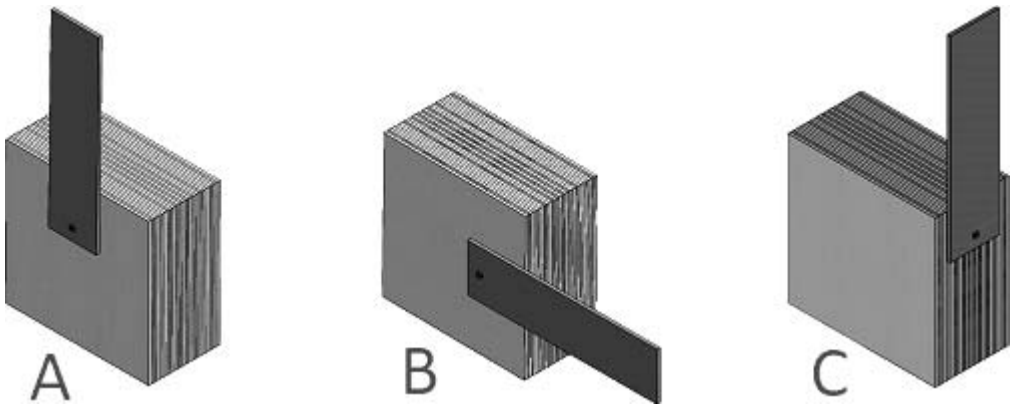

Figure 2.—Illustration of lateral resistance samples, with the three sample orientations.

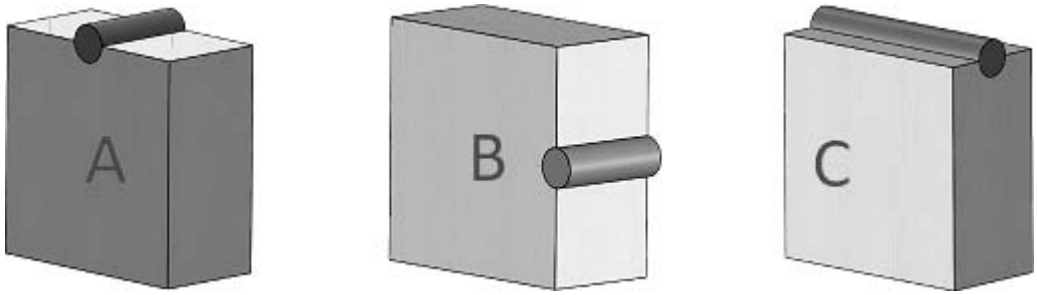

Figure 3.—Illustration of sample containing the half-hole, with the three sample orientations.

length, main-member dowel length, and the dowel-bending yield strength. The SG used for these calculations was experimentally determined as 0.53.

Statistical analysis

A statistical analysis was conducted on the withdrawal, lateral resistance, and dowel-bearing results to understand the behavior of the different orientations. To check the assumptions of normality and equal variance, a Fligner-Killeen test of homogeneity of variances and Shapiro-Wilk normality test were performed. The withdrawal and nail dowel-bearing data were analyzed using an analysis of variance (ANOVA, $\alpha = 0.05$) in the computer software (Program R Version 3.4.3 11-30-2017). Once the ANOVA test was conducted, a Tukey test was used to determine which orientations were significantly different.

Component testing

Component testing was conducted using three connection systems representing a wall-to-floor connection. Two types of angle bracket connectors—Simpson Strong-Tie models HGA10KT and ABR105—were used along with a third configuration, which was a toenail-oriented Simpson Strong-Tie Model SDWS22400DBMB 6'' exterior structural screw to connect the specimens. The ABR105 bracket fasteners used CNA nails, while the HGA10KT bracket fasteners used SDS25300 screws to fabricate the specimen. The ABR105 and the CNA nail system and the HGA10KT bracket and SDS screw systems are referred to as the nail bracket and the screw bracket, respectively. The connection configurations were tested in two directions, shear and withdrawal. Six specimens were tested for each connection configuration and loading direction, for a total of 36 specimens. The test specimens for both directions using all three fasteners can be seen in Figure 5.

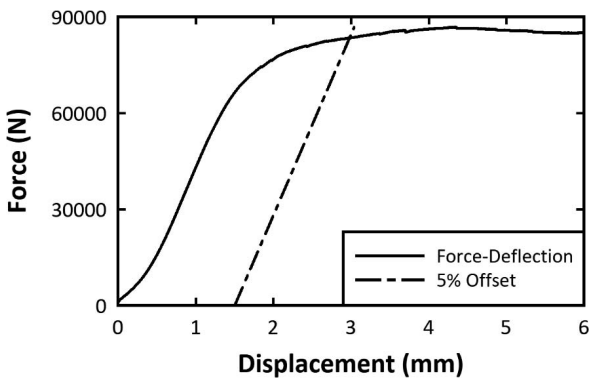

Figure 4.—Load-deflection curve with the 5 percent offset line applied.

Testing was conducted using an MTS 407 Hydraulic Controller attached to an MTS 160 kN Hydraulic Actuator (Model # 244.23) on an MTS Load Unit test bed with a modified loading head. For both testing directions the wall panel was fully braced within the loading fixture, while the floor panel was clamped to the testing bed with C-clamps and a variety of T-slot mounting clamps (Fig. 6).

Both test directions—shear and withdrawal—used the same loading fixture with modifications based on testing directions to the bottom support braces, which were made of 25.4-mm-thick structural-grade rectangular tubing. For the withdrawal testing, the floor panel was clamped flat, making it parallel to the testing bed, and used two 50.8-mm-wide by 165-mm-long bottom support braces under the two overhanging ends of the wall panel (Fig. 7).

During shear testing, the specimens were tested on their sides to create a shear effect in the fastener. The floor panel was clamped vertically to make it perpendicular to the testing bed and used two 50.8-mm-wide by 330-mm-long bottom support braces under the overhanging wall panel (Fig. 8).

The two monotonic tests were performed for each connection system with a displacement rate of 6.35 mm/min until failure. The monotonic tests were used to calculate the estimated failure displacement for cyclic testing, which is related to the Consortium of Universities for Research in Earthquake Engineering (CUREE) reference displacement (Δ). Four cyclic tests were performed for each connection system using the CUREE displacement control protocol (Krawinkler et al. 2001). The modified CUREE displacement protocol can be seen in Figure 9, scaled as a ratio of the reference displacement (Δ). The reference displacement was determined following the procedure outlined in Langlois et al. (2004), resulting in CUREE reference displacements of 22.9, 16.5, and 19.1 mm for the nails, screws, and toe screws, respectively.

The lateral cyclic tests used the standard CUREE displacement protocol, whereas the withdrawal tests required a modification in displacement protocol. This involved a one-sided CUREE protocol, with only positive displacements, because the purpose of the test was to determine the withdrawal behavior of the connection, not the withdrawal and bearing properties. The reference displacement for these tests was 11.4 mm for the first two toe screw samples and 12.7 mm for all other tests. This modification to the abbreviated CUREE displacement protocol can be seen in Figure 9b.

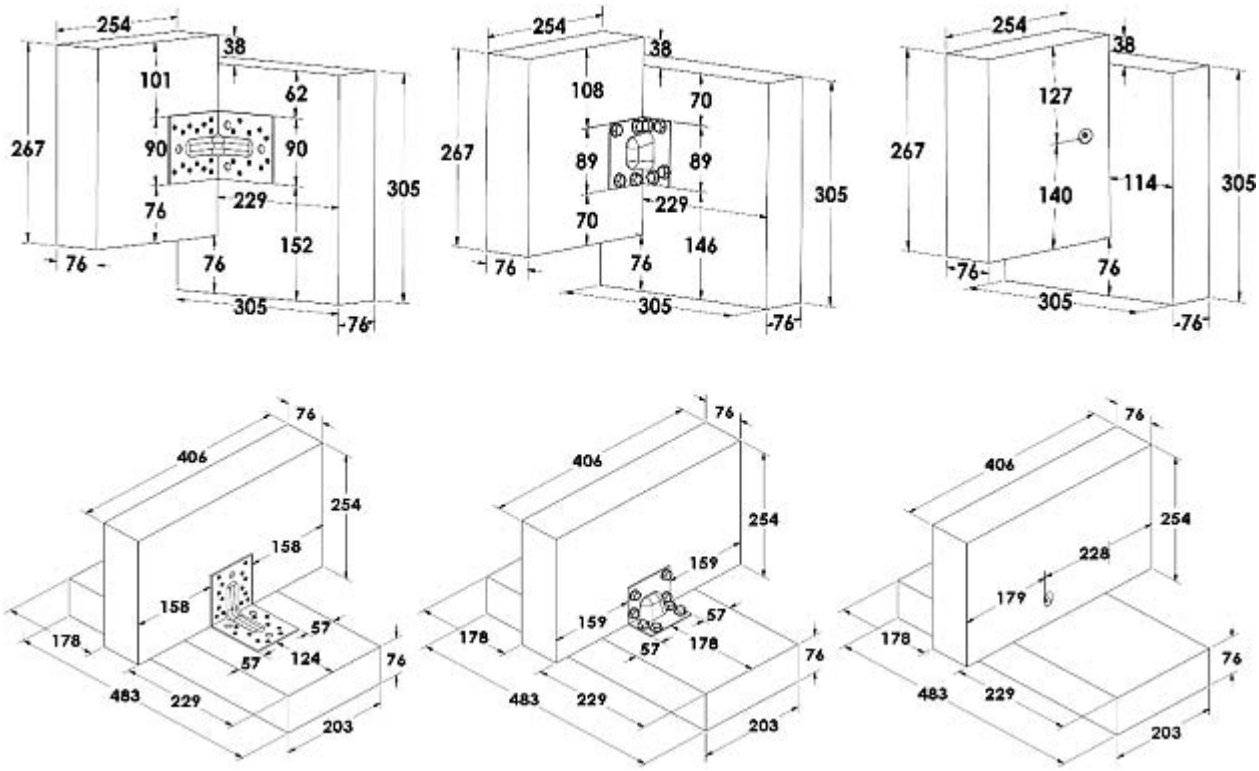

Figure 5.—Shear samples (top) with ABR, HGA, and toe screw (right to left). All dimensions are in millimeters (mm). Withdrawal samples (bottom) with ABR, HGA, and toe screw (right to left). All dimensions are in millimeters (mm).

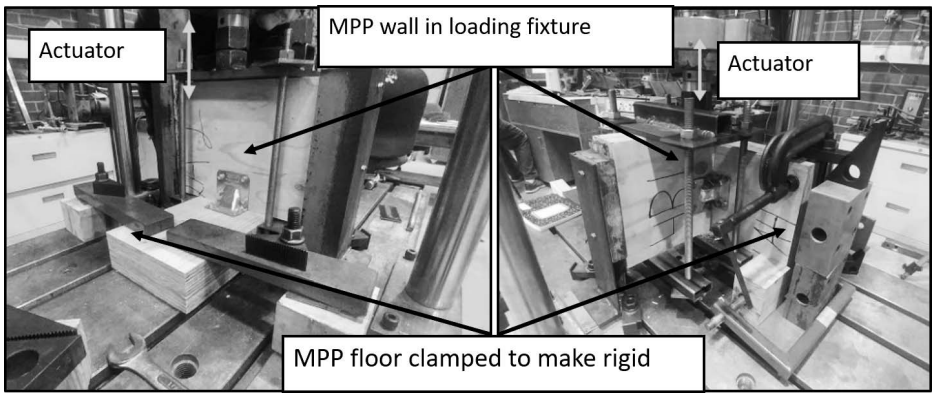

Figure 6.—(Left) withdrawal direction testing setup; and (right) shear direction testing setup.

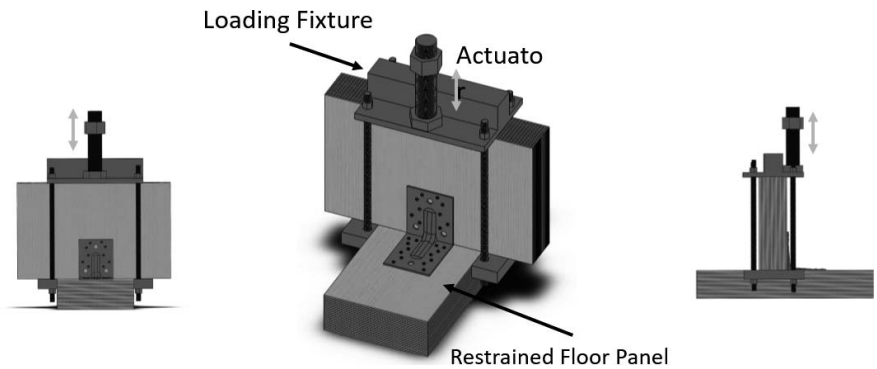

Figure 7.—Testing setup in the withdrawal direction without clamping of the floor panel.

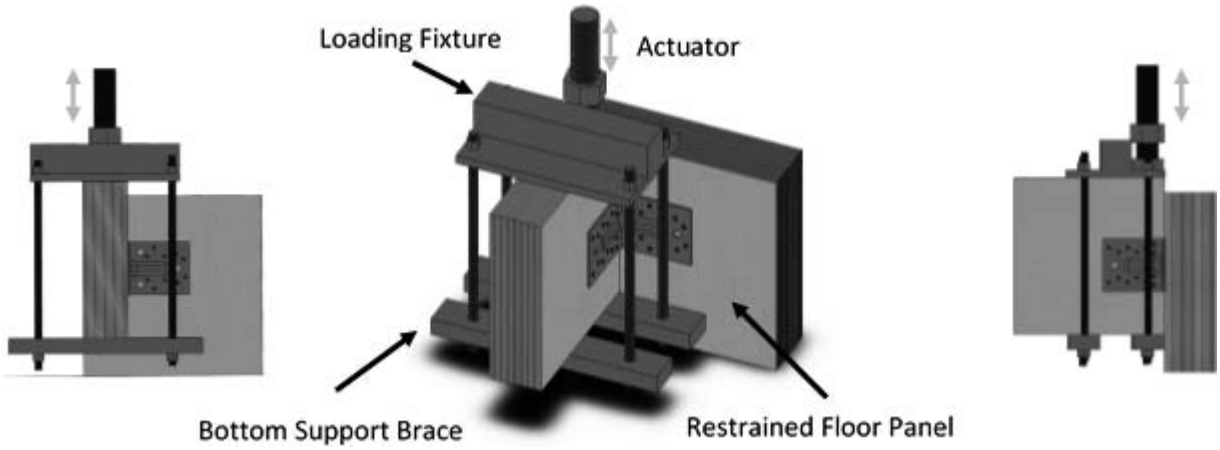

Figure 8.—Testing setup in the shear direction without clamping of the floor panel.

Results and Discussion

Withdrawal

The average withdrawal capacity of the fasteners installed into the face of the panel (Orientation A) was 58 N/mm (coefficient of variation [COV] = 7%) for the 8D smooth shank nails, 75 N/mm (COV = 9%) for the CNA ring shank nails, and 163 N/mm (COV = 10%) for the SDS screws (Table 2). As expected, the screws had a greater maximum holding capacity. Orientations B and C for all the fastener types were consistently lower than Orientation A (Table 2).

There was a significant difference in mean withdrawal resistance (Smooth, Ring, and Screw: ANOVA $P < 0.05$) between orientations. The three fastener types showed similar orientation effects on the withdrawal capacity. Orientation A withdrawal capacity for all the fasteners had strong evidence that it differed from both Orientations B and C (Smooth, Ring, Screw: all Tukey $P < 0.05$), while there was no evidence that withdrawal capacity in Orientations B and C differed (Smooth, Ring, Screw: all Tukey $P > 0.5$; Table 2).

The COV for withdrawal capacity in Orientations B and C did appear large with a range from 18 to 33 percent (Table 2), which can be explained by the installation location. The fastener may have passed through two or three plies or could have gone directly through a bond line depending on the fastener location; hence, the greater variability.

Using the empirical equations for withdrawal resistance in solid sawn lumber from the Wood Handbook resulted in wood screw values of 84 N/mm, while the predicted values for the lag screws were 197 N/mm through the face and 148 N/mm through the end grain or plies (FPL 2010). The higher prediction values were expected because the equation accounted for solid sawn lumber and not plywood. Plywood has been known to have 15 to 30 percent lower withdrawal resistance than solid lumber, which can be seen with the test values (FPL 2010). Similarly, Mahdavifar et al. (2018) reported 4 and 14 percent lower withdrawal values for nails and screws, respectively.

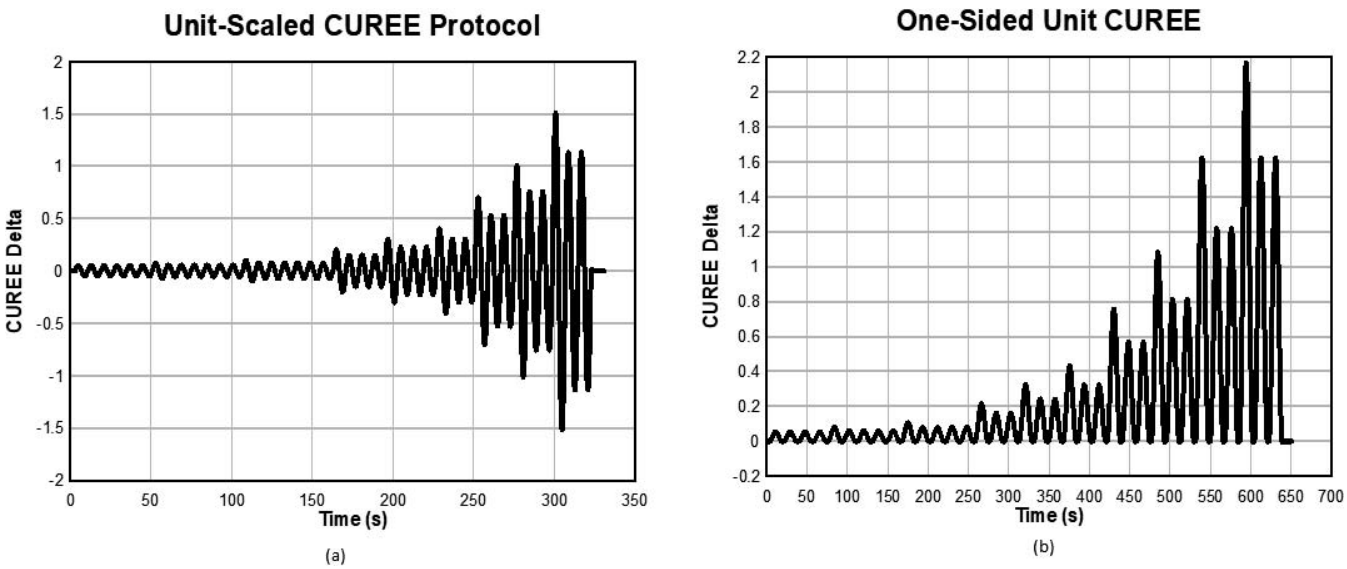

Figure 9.—Consortium of Universities for Research in Earthquake Engineering (CUREE) displacement protocols. (a) CUREE used on shear specimens; (b) one-sided abbreviated CUREE used on specimens loaded in withdrawal.

Table 2.—Single fastener testing results: withdrawal, lateral resistance, and dowel bearing.[a,b]

Test	Fastener	Orientation A		Orientation B		Orientation C	
		Average	COV (%)	Average	COV (%)	Average	COV (%)
Withdrawal (N/mm)	8D	58 A	7	30 B	26	29 B	24
	CNA	75 A	9	39 B	19	36 B	33
	SDS	163 A	10	101 B	18	115 B	18
Lateral (N)	CNA	1,743 A	10	2,183 A	31	1,151 B	19
	SDS	4,252 A	19	4,834 A	7	1,951 B	31
Dowel bearing (MPa)	CNA	45 A	24	38 A	28	18 B	40
	SDS	44 A	9	39 A	5	12 B	20
	12.7 mm	38 A	6	34 A	7	—	—
	25.4 mm	42 A	7	35 A	4	—	—

[a] COV = coefficient of variation.

[b] A and B represent the statistical significance between the orientations. If the orientations have the same letter, they are statistically similar; if they have different letters, they are statistically different.

Lateral resistance test

The average yield load for the nails installed in Orientation A was 1,743 N (COV = 10%), while Orientation B had an average of 2,183 N (COV = 31%; Table 2). The results for Douglas-fir CLT and CNA nails with similar steel plate were lower (1,592 N; Mahdavifar et al. 2018) than that of MPP (1,743 N; Table 2). Orientation C had the lowest yield load average of 1,151 N (COV = 19%; Table 2). There was evidence of a difference (Kruskal-Wallis, $P = 0.002$) between the mean ranks of at least one pair of groups. A relatively higher yield load was observed for Orientations A and B when compared with Orientation C, which was expected as a result of the fastener being installed between the plies (Table 2). When the fastener was loaded in Orientation C, many of the MPP samples would split at a bond line and would continue to propagate as the testing continued. Orientation B had a high COV, as well as some higher yield loads than Orientation A, which could be due to how the fasteners were loaded in the MPP. In Orientation A, the fastener was loaded parallel-to-grain in the face plies, which caused a splitting of the plies. In Orientation B, the fastener was loaded perpendicular-to-grain of the face plies, which caused a crushing failure of the face plies and increased the yield loads.

The yield modes for Orientations A and B were III_s, which is indicated by a plastic hinge yield of the fastener between the main and side members as well as wood bearing failure (AWC 2018). The occurrence of deformation or damage of the MPP (main member) was minimal, while little to no damage occurred within the steel side member. The yield mode for Orientation C was a III_m, which is similar to a III_s but involves more crushing within the MPP (main member). The calculated EYM compared the MPP with three values; the first two were calculated using dowel-bearing strengths of NDS tabulated values for plywood and wood species with the SG of 0.53. Using these values, the EYM estimated an expected III_s yield mode with minimum yield loads of 1,802 and 1,883 N, for the SG of 0.53 and plywood, respectively. The third comparison was the observed value, which was calculated using the average test value for dowel bearing, and the estimated III_s yield mode with a minimum value of 1,938 N. The estimated yield modes and loads were similar to Orientations A and B, with the yield loads falling between both orientations' averages. The EYM did not account for installation of the nail within the side of the MPP (Orientation C), which could be considered end grain and is not permitted by the NDS.

The average yield loads for the screws installed in Orientations A and B were 4,252 N (COV = 19%) and 4,834 N (COV = 7%), respectively, while Orientation C had the lowest average yield load of 1,915 N (COV = 31%; Table 2).

The screws had similar failure results to the nail lateral resistance tests. The lateral yield strength was greater for screws than Douglas-fir CLT (3,462 N; Mahdavifar et al. 2018). Orientation C had the lowest yielding loads, which was expected. During testing, the screws in Orientation A caused the face plies to split, while in Orientation B crushing of the face plies occurred, similar to that of the nail tests. Unlike the nail tests, Orientation B had a low COV, but still had a slightly higher yield average. The lower COV could be a result of an increased diameter of the fastener.

The yield modes for the screws were similar to those of the nails, with Orientations A and B having yield modes of III_s. The occurrence of deformation of the MPP (main member) was minimal, while yielding of the steel (side member) occurred around the screw head. The yield mode for Orientation C was a III_m, with more deformation occurring in the MPP. Using the same comparison as the CNA nails, the EYM for the SDS screws estimated an expected III_s yield mode with minimum yield loads of 4,693 and 4,192 N for the SG of 0.53 and plywood, respectively. The observed value estimated a III_s yield mode with a minimum value of 4,586 N. The estimated yield modes and loads were similar for Orientations A and B, with the yield loads falling between both orientations' averages. Again, the EYM did not account for installation of the nail within the side of the MPP (Orientation C).

Dowel bearing

The dowel-bearing strength of MPP in Orientation A was similar to common structural wood species in the United States, but had greater dowel-bearing strengths in Orientation B (Wilkinson 1991, Rammer and Winistorfer 2001, Kent et al. 2004, AWC 2018). The dowels that were loaded along the plies (Orientation C) were particularly low, which could be comparable to end-grain. Orientations A and B were statistically similar ($P > 0.05$; Table 2) through all dowel diameters, while Orientation C statistically differed ($P < 0.05$; Table 2). MPP dowel-bearing strengths in both the A and B Orientations were similar and/or greater when

compared with engineered wood products such as laminated veneer lumber (LVL) and oriented strand lumber (Avent and Alawady 1999, Hwang and Komatsu 2002). MPP is similar to LVL in dowel-bearing properties in the parallel orientation, but MPP's dowel-bearing strength is considerably greater in the perpendicular direction because of its cross plies.

The nail samples with diameters of 4 mm contained some specimens for which the 5 percent yield limit could not be calculated because of the linearity of the graph, causing the offset to not intersect the curve. For these samples the method from Wilkinson (1991) was used by using the maximum load as the 5 percent offset load. This produced higher yield loads and variability in the data. The average strengths for the two directions going through the plies (Orientations A and B) were 45 and 38 MPa (COV = 28% and 39%), respectively. The dowel-bearing averages were higher than the NDS tabulated values of 36 MPa for SG = 0.53 of a wood member, and 32 MPa for SG = 0.5 of structural plywood (AWC 2018, tables 12.3.3 and 12.3.3B). The Along Ply (Orientation C) had the lowest dowel-bearing strength, with an average of 18 MPa (COV = 40%; Table 2). The lower strength and greater variation in Orientation C was caused by varying failure types, either crushing or splitting. The crushing failure occurred by the dowel crushing the plies on which it was installed, whereas the splitting occurred if the dowel was installed closer to a glue line, causing the sample to split.

The average screw dowel-bearing strengths of the two directions going through the plies (Orientations A and B) were 44 and 39 MPa (COV = 9% and 5%; Table 2), respectively. The dowel-bearing strength of Orientation A was similar to the NDS tabulated value of 41 MPa, whereas the dowel-bearing strength of Orientation B was slightly greater than the NDS tabulated value of 33 MPa (NDS table 12.3.3; AWC 2018). Both the directions showed larger values when compared with the NDS predicted value for plywood of 32 MPa. The average strength for Orientation C was 12 MPa (COV = 20%; Table 2), which could be explained by the varying failure types, similar to the nails.

The 12.7- and 24.5-mm-diameter dowels only had two orientations tested, Orientations A and B. The 25.4-mm samples averaged 42 and 35 MPa (COV = 7% and 4%) in Orientations A and B, respectively (Table 2). The dowel-bearing strength for Orientation A was similar to the NDS tabulated value of 41 MPa, whereas Orientation B for the observed dowel-bearing strength was much greater than the predicted value of 17 MPa (NDS table 12.3.3; AWC 2018). The 12.7-mm samples averaged 38 and 34 MPa (COV = 6% and 7%) in Orientations A and B, respectively (Table 2). The dowel-bearing strength for Orientation A was similar to the NDS tabulated value of 41 MPa, whereas Orientation B for the observed dowel-bearing strength was much greater than the predicted value of 24 MPa (NDS table 12.3.3; AWC 2018).

Component tests

The nail bracket connection had an average capacity of 24 kN in shear-dominated loading direction and 27 kN in withdrawal-dominated loading direction (Table 3). The screw bracket connection had an average capacity of 23 kN in shear and 25 kN in withdrawal (Table 3). The nail bracket exhibited greater capacities in both directions than the screw bracket, but the screw bracket had greater initial stiffness and energy dissipation qualities than the nail bracket (Table 3). Douglas-fir CLT with similar screw brackets had a capacity of 14.6 kN in shear and 13.1 kN in withdrawal; and similarly, the performance of CLT with nail brackets was 20 and 20.81 kN in shear and withdrawal loading, respectively (Mahdavifar et al. 2019). As is evident from the comparison of results with Mahdavifar et al. (2019), the MPP connections performed substantially better. The toe screw connection had an average capacity of 13 kN in shear and 26 kN in withdrawal (Table 3). Of interest with the toe screw was the failure mode in withdrawal; two specimens exhibited failure of the screw in withdrawal, while the other specimens exhibited steel failure of one of the two screws, followed by pull-through of the other screw. The stiffness shown is the initial stiffness of the connection.

Table 3.—Cyclic connection results.[a]

Test	Fastener	Strength (kN)	Displacement (mm)	Stiffness (kN/cm)
Shear	Nail (CAN)	24	22	27
	COV (%)	9	1	14
	Screw (SDS)	23	10	63
	COV (%)	3	9	8
	Toe screw	13	12	39
	COV (%)	20	5	20
Withdrawal	Nail (CAN)	27	14	40
	COV (%)	9	4	20
	Screw (SDS)	25	18	62
	COV (%)	4	6	10
	Toe screw	26	18	56
	COV (%)	1	10	51

[a] COV = coefficient of variation.

In addition to the tabulated results, investigation of the hysteretic results (Fig. 10) showed interesting trends, especially for energy dissipation (Table 4). The equivalent viscous damping was calculated on a per-cycle basis, with the highest values being from a leading cycle shown. The screw resulted in the highest equivalent viscous damping in shear, while the toe screws resulted in the highest value for withdrawal. The nails had the lowest damping. The screws dissipated the most energy, both on a per-cycle and total energy basis (Table 4). The toe screws, while they had a higher damping ratio than the nails, had the lowest energy dissipated on a per-cycle basis as well as total energy metric.

Models

The application of engineering material models to the experimental results can be beneficial for numerical modeling and design. As such, the parameters for two different material models were determined from the hysteretic results of the component testing—the American Society of Civil Engineers (ASCE) 41-13 trilinear curve and seismic analysis of wood-frame structures (SAWS) model parameters.

The ASCE 41-13 trilinear curve comes from the nonlinear static procedure in ASCE 41-13 (2013), which pertains to analysis of existing structures for seismic events. The curve is constructed from three lines taken from the backbone of the hysteretic data. The procedure uses an assumption that a yield point exists which is a fraction of the maximum force, and two lines relating to the yield point

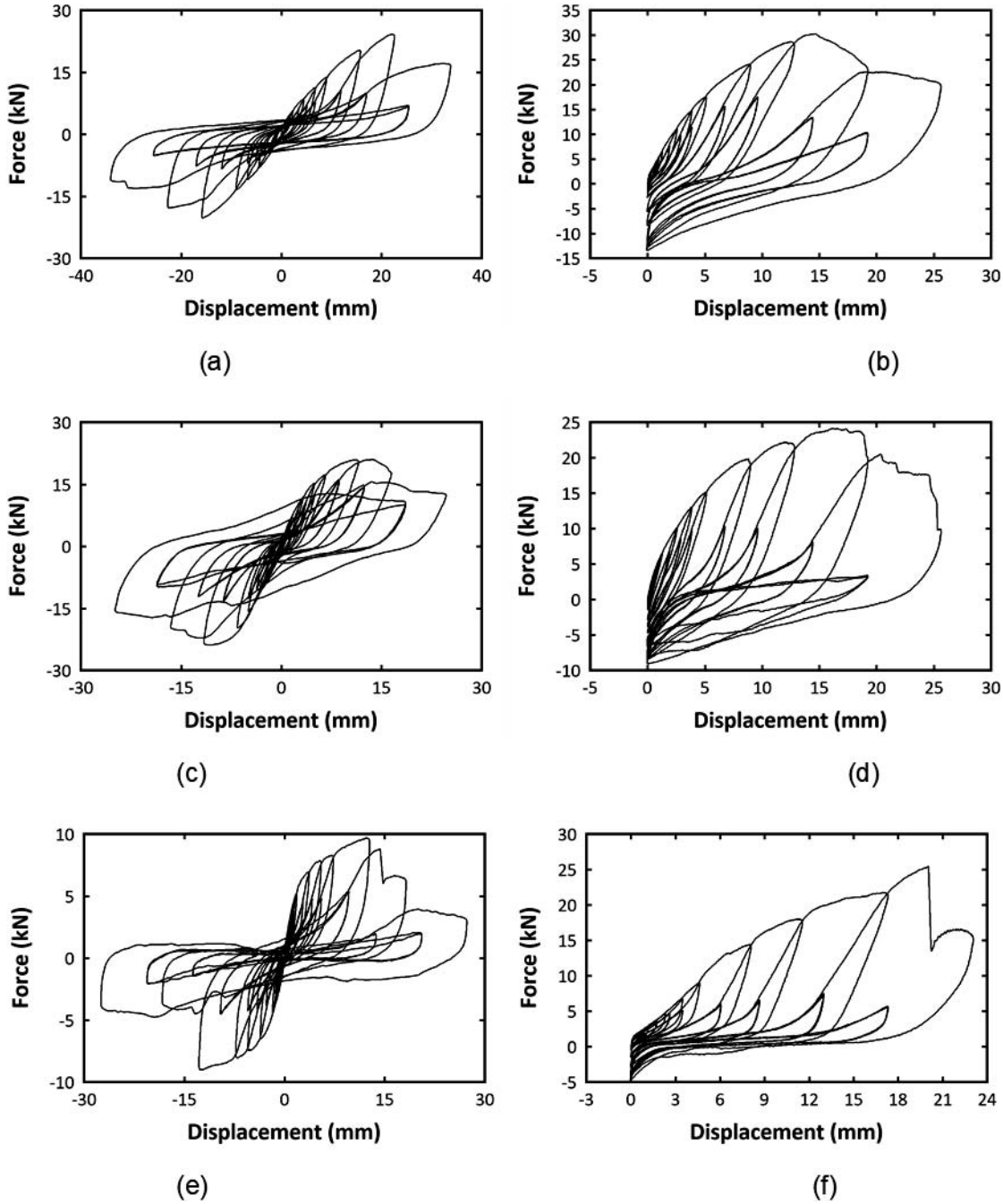

Figure 10.—Representative hystereses and backbones from each connector in shear and withdrawal. (a) and (b), nail in shear and withdrawal, respectively; (c) and (d), screw in shear and withdrawal, respectively; (e) and (f), toe screw in shear and withdrawal, respectively.

will result in an energy balance between the two lines and the backbone up to maximum load. The third linear portion is from the point on the load-displacement curve of maximum force and displacement to a point associated with 60 percent of the determined yield load and associated displacement to the postpeak region of the curve or the last experimental point if the test ends prior to 60 percent of the determined yield. This limitation on the third linear portion occurred due to the test ending prior to degradation to < 60 percent of the yield, because the yield is not a known constant prior to testing.

Tabulated results of the modeling parameters are presented in Table 5. The model outputs are compared against their respective experimental results in Figure 11. The yield strength (Fy) and ultimate strength (FU) are fairly consistent within each sample, with the exception of the yield strength of both toe screw samples and the ultimate strength of the toe screw in shear. The stiffness parameters varied much more for the toe screw samples. The three stiffness terms, K, a1K, and a2K, represent the stiffness of the preyield, postyield, and postpeak stiffness, respectively. The toe screws exhibited the largest COV for stiffness.

Table 4.—Average energy dissipation results for connector tests.[a]

Test	Connector	Equivalent viscous damping (%)	Maximum energy in one cycle (j)	Total energy (j)
Shear	Nail	22.7	634	2,863
	COV (%)	7.60	13	10.80
	Screw	33	755	3,146
	COV (%)	8.50	3.40	7.50
	Toe screw	37.3	226	1,275
	COV (%)	61.70	13.10	17.90
Withdrawal	Nail	17.5	296	1,036
	COV (%)	6.40	12.80	13.90
	Screw	26.4	348	1,081
	COV (%)	38.10	23.80	5.30
	Toe screw	16.2	189	601
	COV (%)	34.70	8.60	15.20

[a] COV = coefficient of variation.

Table 5.—American Society of Civil Engineers 41-13 trilinear parameters, average and COV.[a]

Test	Fastener	Fy (kN)	FU (kN)	K (kN/mm)	a1 × K (kN/mm)	a2 × K (kN/mm)
Shear	Nail (CNA)	16	24	1.8	0.58	−0.92
	COV (%)	9	9	7	22	18
	Screw (SDS)	17	22	4.6	0.63	−0.68
	COV (%)	5	2	11	29	11
	Toe screw	9	13	4.5	0.45	−1.36
	COV (%)	16	20	30	34	23
Withdrawal	Nail (CNA)	18	27	3.8	0.97	−0.79
	COV (%)	12	9	9	12	17
	Screw (SDS)	16	25	4.1	0.63	−1.54
	COV (%)	6	4	19	6	38
	Toe screw	14	26	4.9	0.83	−8.81
	COV (%)	14	1	61	12	147

[a] COV = coefficient of variation; Fy = yield strength; FU = ultimate strength; K = preyield stiffness; a1 × K = postyield stiffness; a2 × K = postpeak stiffness.

The SAWS model parameters are more complex and model the entire hysteretic behavior of the connection (Folz and Filiatrault 2004). The SAWS model was created for wood-frame walls, but many of its pinching characteristics allow for it to model connectors in wood with acceptable accuracy. There are 10 different parameters in the SAWS model; five are extracted from the envelope of the hysteretic response, while five model the unloading, reloading, and degradation of the material. The parameters for SAWS were determined using a modified version of the method described in Mahdavifar (2017). This method involves determining initial values from the curve and then optimizing these values using simulated annealing. The backbone values were optimized using the equations from Folz and Filiatrault (2004), with the simulated annealing minimizing for the percent difference in load at all points. The other five variables were determined using Open Sees to run the entire experimental results and minimizing the energy difference between the model and the experimental data (McKenna et al. 2000). The tabulated mean results can be seen in Table 6, while the resultant hysteresis for one set of model parameters overlaid over the experimental data can be seen in Figure 12. Some issues of fit did occur for certain trials where the SAWS material would encounter a failure criterion. When the pinching portion of the path intersects with the defined backbone, SAWS recognizes this as failure and causes all subsequent forces to be output as zero (Shen et al. 2013).

Table 6.—Average estimated seismic analysis of wood-frame structures (SAWS) parameters.[a]

Fastener	F1 (kN)	F0 (kN)	DU (mm)	So (kN/mm)	R1	R2	R3	R4	a	b
Nail shear	13.8	3.5	21.9	3.88	0.091	−0.238	0.706	0.060	0.418	1.161
COV (%)	43.2	22.8	1.2	28.7	65.1	22.8	15.9	83.5	56.8	9.2
Screw shear	16.0	2.8	10.6	8.02	0.070	−0.086	1.164	0.106	0.909	2.530
COV (%)	4.6	97.1	7.7	8.9	37.8	15.7	9.2	37.6	41.6	8.5
Toe screw shear	8.7	3.2	11.7	7.20	0.041	−0.080	0.713	0.059	0.853	1.293
COV (%)	35.7	47.9	4.3	16.6	83.5	11.6	36.2	67.1	22.1	8.3

[a] COV = coefficient of variation. For detailed information on the standard SAWS parameters listed here, see Folz and Filiatrault (2004).

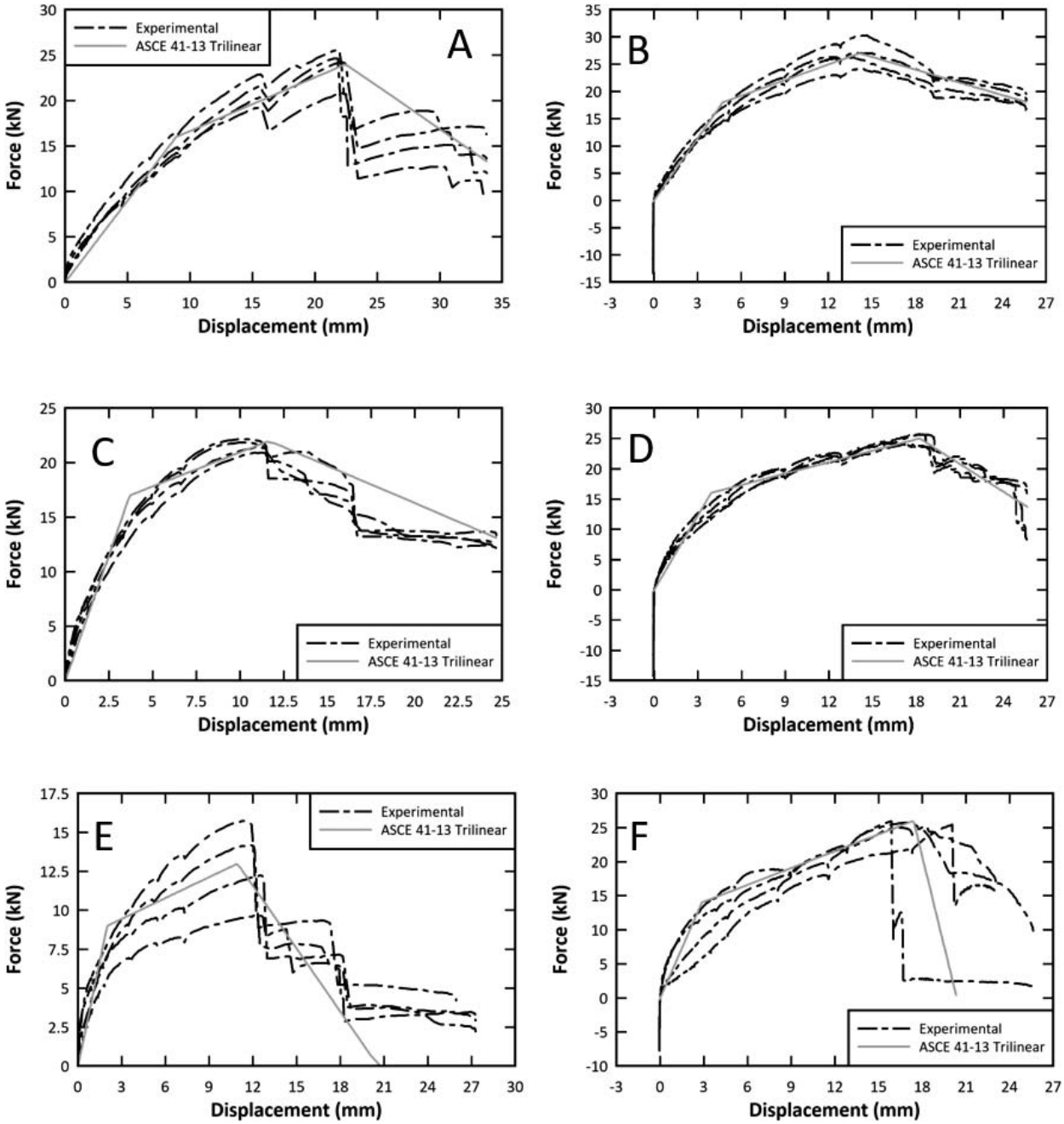

Figure 11.—American Society of Civil Engineers (ASCE) 41-13 trilinear average models with related backbone curves. (A), (C), and (E) show the shear specimens for the nails, screws, and toe screws, respectively. (B), (D), and (F) show the withdrawal specimens for the nails, screws, and toe screws, respectively.

Conclusion

This study was conducted to understand the mechanical properties of MPP for structural use. The tests that were conducted were fastener withdrawal resistance, dowel-bearing strength, lateral resistance, and a component test on a wall-to-floor system connection.

A variety of fastener tests were conducted to indicate whether the NDS could properly predict the withdrawal, lateral resistance, and dowel-bearing strengths. The withdrawal capacity was low, because the empirical equations accounted for solid sawn lumber and not plywood. Once a 15 percent reduction was incorporated within the predicted values, they became similar to the observed values. The lateral resistance test indicated that the EYM could be used to calculate the yield loads and yield mode of the MPP by using the dowel-bearing strength of plywood. The dowel-bearing strength of MPP was also calculated and resulted in similar values in the parallel orientation to the tabulated NDS values for a wood member with an SG of 0.53. The NDS tabulated values were notably low for the perpendicular orientation, due to the cross-plies of MPP. MPP in Orientation C and along the plies displayed low strengths and were not able to be predicted in the EYM and NDS.

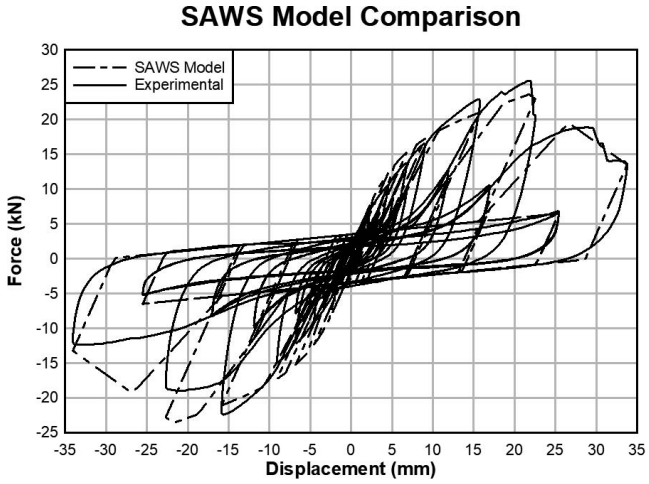

Figure 12.—Seismic analysis of wood-frame structures (SAWS) model fit for specimen N2.

Three different component assemblies were tested in two distinct loading directions. The connection with ABR brackets and HGA10KT brackets performed similarly in terms of strength. However, HGA bracket connections had greater stiffness in both shear and withdrawal loading directions. The toe screw connection expectedly is weaker in shear loading direction but has comparable strength in withdrawal loading configuration. The small specimen test results provided adequate data for modeling, which will be useful for describing MPP behavior for lateral and withdrawal loads. These models were the ASCE 41 tri-linear curve and SAWS 10 parameter model. The SAWS model does not describe the behavior well for all cases. For engineers, the ASCE 41 model is adequate for use.

Acknowledgments

The authors would like to thank US Economic Development Agency, which funded this work, as well as the TallWood Design Institute.

Literature Cited

American Society of Civil Engineers (ASCE). 2013. Seismic rehabilitation of existing buildings. ASCE 41-13. ASCE, Reston, Virginia.

American Wood Council (AWC). 2015. General dowel equations for calculating lateral connection values. AWC, Washington, D.C.

American Wood Council (AWC). 2018. National design specification® for wood construction. AWC, Washington, D.C.

APA—The Engineered Wood Association. 2018a. Product report. Freres mass plywood panel products. PR-L325. APA, Tacoma, Washington.

ASTM International. 2012. Standard test method for mechanical fasteners in wood. ASTM D1761. ASTM International, West Conshohocken, Pennsylvania.

ASTM International. 2018. Standard test method for evaluating dowel-bearing strength of wood and wood-base products. ASTM D5764. ASTM International, West Conshohocken, Pennsylvania.

Avent, R.R. and M. Alawady (Eds). 1999. Structural Engineering in the 21st Century. American Society of Civil Engineers, Reston, Virginia. pp. 626–630.

Ceccotti, A., C. Sandhaas, M. Okabe, M. Yasumura, C. Minowa, and N. Kawai. 2013. SOFIE project—3D shaking table test on a seven-storey full-scale cross-laminated timber building. *Earthq. Eng. Struc. Dyn.* 42(13):2003–2021.

Folz, B. and A. Filiatrault. 2004. Seismic analysis of woodframe structures I: Model formulation. *J. Struct. Eng.* 130(9):1353–1360.

Forest Products Laboratory (FPL). 2010. Wood handbook—Wood as an engineering material. General Technical Report FPL-GTR-190. USDA Forest Service, FPL, Madison, Wisconsin. 508 pp.

Gavric, I., A. Ceccotti, and M. Fragiacomo. 2011. Experimental cyclic tests on cross-laminated timber panels and typical connections. Presented at the 14th ANIDIS Conference, September 18–22, 2011, Bari, Italy.

Hwang, K. and K. Komatsu. 2002. Bearing properties of engineered wood products 1: Effects of dowel diameter and loading direction. *J. Wood Sci.* 48:295–301.

Kent, S. M., R. J. Leichti, D. V. Rosowsky, and J. J. Morrell 2004. Effect of wood decay by *Postia placenta* on the lateral capacity of nailed oriented strandboard sheathing and Douglas-fir framing members. *Wood Fiber Sci.* 36(4):560–572.

Kramer, A., A. R. Barbosa, and A. Sinha. 2015. Performance of steel energy dissipaters connected to cross-laminated timber wall panels subjected to tension and cyclic loading. *ASCE J. Struct. Eng.* 142(4):E4015013. DOI:10.1061/(ASCE)ST.1943-541X.0001410

Krawinkler, H., F. Parisi, L. Ibarra, A. Ayoub, and R. Medina 2001. Development of a testing protocol for wood frame structures. CUREE-Caltech Woodframe Project Report No. W-02. Stanford University, Palo Alto, California.

Kremer, P. D. and M. A. Symmons. 2015. Mass timber construction as an alternative to concrete and steel in the Australia building industry: A PESTEL evaluation of the potential. *Int. Wood Prod. J.* 6(3):138–147.

Langlois, J. D., R. Gupta, and T. H. Miller. 2004. Effects of reference displacement and damage accumulation in wood shear walls. *J. Struct. Eng.* 130(3):470–479.

Mahdavifar, V. 2017. Cyclic performance of connections used in hybrid cross-laminated timber. Doctoral dissertation. Oregon State University, Corvallis.

Mahdavifar, V., A. R. Barbosa, A. Sinha, L. M. Muszynski, and R. Gupta. 2016. Hysteretic behaviour of metal connectors for hybrid (high- and low-grade mixed species) cross laminated timber. Presented at the 2016 World Conference on Timber Engineering, August 22–25, 2016, Vienna, Austria.

Mahdavifar, V., A. R. Barbosa, A. Sinha, L. M. Muszynski, and R. Gupta. 2018. Lateral and withdrawal capacity of fasteners on hybrid cross-laminated timber panels. *ASCE J. Mat. Civ. Eng.* 30(9). DOI:10.1061/(ASCE)MT.1943-5533.0002432

Mahdavifar, V., A. R. Barbosa, A. Sinha, L. Muszynski, R. Gupta, and S. Pryor. 2019. Hysteretic response of metal connections on hybrid cross-laminated timber panels. *J. Struct. Eng.* 145(1):04018237.

McKenna, F., G. L. Fenves, and M. H. Scott. 2000. Open system for earthquake engineering simulation. University of California, Berkeley. http://opensees.berkeley.edu. Accessed December 6, 2000.

Pei, S., J. van de Lindt, and M. Popovski. 2013. Approximate R-Factor for cross-laminated timber walls in multistory buildings. *J. Archit. Eng.* 13(19):245–255. DOI:10.1061/(ASCE)AE.1943-5568.0000117

Rammer, D. R. and S. G. Winistorfer. 2001. Effect of moisture content of dowel-bearing strength. *Wood Fiber Sci.* 33(1):126–139.

Rinaldin, G., C. Amadio, and M. Fragiacomo. 2013. A component approach for the hysteretic behavior of connections in cross-laminated wooden structures. *Earthq. Eng. Struct. Dyn.* 13(42):2023–2042.

Shen, Y., J. Schneider, S. Tesfamariam, S. Stiemer, and Z. Mu. 2013. Hysteresis behavior of bracket connection in cross-laminated-timber shear walls. *Construct. Build. Mater.* 48:980–991.

Wilkinson, T. 1991. Dowel bearing strength. Research Paper FPL-RP-505. USDA Forest Service, Forest Products Laboratory, Madison, Wisconsin.